PHYSICAL REVIEW B, VOLUME 64, 121405(R)

# Catalyst-free synthesis of boron nitride single-wall nanotubes with a preferred zig-zag configuration

R. S. Lee, J. Gavillet, M. Lamy de la Chapelle, and A. Loiseau
*LEM, ONERA-CNRS, BP72, 92322 Châtillon Cedex, France*

J.-L. Cochon and D. Pigache
*ONERA, 91761 Palaiseau Cedex, France*

J. Thibault
*SP2M, CENG, 38054 Grenoble Cedex 9, France*

F. Willaime
*SRMP, CEA/Saclay, 91191 Gif-sur-Yvette Cedex, France*
(Received 23 February 2001; published 10 September 2001)

Boron nitride nanotubes (BNNTs) were synthesized in gram quantities using a continuous $CO_2$ laser ablation reactor without the benefit of a metal catalyst. High-resolution transmission electron microscopy analyses have shown the samples to be composed of single-wall nanotubes organized in long and well-crystallized bundles containing about ten tubes. The samples also contain a small amount of double-wall BNNTs and multiwall boron nitride fullerenelike ''cages.'' The majority of the BNNTs were identified as having the zig-zag configuration, as attested by the 0.2 nm period array of spots observed along tube walls; the other tubes are either armchair or chiral. The BNNTs seem to be attached at one end to nanoparticles which were shown in electron spectroscopy imaging mode to be composed of pure boron, thus supporting a root-based growth mechanism.

DOI: 10.1103/PhysRevB.64.121405 PACS number(s): 61.46.+w, 68.37.Lp, 81.10.Aj

Since the initial proposition that boron nitride nanotubes (BNNTs) could be stable,[1] they have been successfully synthesized using the same methods as for the production of carbon nanotubes (CNTs), i.e., in particular electric arc discharge and laser ablation of BN targets.[2–10] BNNTs are attractive because their physical properties could complement those of CNTs. BNNTs reportedly have mechanical properties similar to those of CNTs (elastic modulus $\simeq 1.2$ TPa)[8] while their electronic properties are very different, being semiconductors with a wide band gap weakly dependent on helicity and tube radius.[1,9] The relative uniformity of their electronic properties raises the possibility of nanoelectronic applications without the need for helicity selection, which is necessary in the case of CNTs in light of the strong dependence of their electronic properties on helicity.[10]

Until recently, the study of BNNTs has been stymied by the paucity of material produced via the various synthesis paths outlined above. The low quantity of material produced made the characterization of certain physical and chemical properties difficult, if not impossible. Early samples were also highly heterogeneous, being comprised of BNNTs with varying numbers of coaxial cylinders,[3,11] except in the case of Ref. 7, where the vast majority of tubes were double-walled.

We have synthesized BNNTs in ''bulk'' quantities using a continuous laser ablation reactor.[12] A rotating catalyst-free BN target (diameter $\simeq 6.5$ mm)[13] was ablated with a $CO_2$ laser ($\lambda = 10.6 \mu$m, 1 kW) focused to 7.5 mm. The reaction was carried out in a 1 bar nitrogen atmosphere; a 100 ml/s nitrogen flow carried the ablated material out of the reaction chamber where it was collected in a trap and filter. The average temperature of the target during ablation was measured via optical pyrometry to be about 3400 K. The elevation of the target was manually adjusted to allow for continuous ablation. The optimization of the synthesis conditions allowed to obtain gram quantities of product; this was made possible by an increase of the yield for BNNT production ($\simeq 0.6$ g/h) by several orders of magnitudes with respect to previous syntheses. The reaction product collected from the trap and filter was, respectively, a light beige and a dense gray film. The samples were sonicated in ethanol and dispersed on holey carbon film 300 mesh copper grids prior to being examined using a transmission electron microscope. Despite the difference in the macroscopic appearance of the samples collected from the trap and filter, no discernable difference was evident in their transmission electron micrographs (TEMs).

Figure 1 shows some typical micrographs of the recovered material taken using a JEOL 4000FX TEM. A low-magnification micrograph [Fig. 1(A)] shows that the majority of the sample is composed of single-wall nanotubes (SWNTs) with some multi-wall (primarily double-wall) nanotubes and particles encapsulated by multi-wall fullerenelike structures. Most of the SWNTs are organized in small bundles [Fig. 1(B)] made of about 10 tubes although some isolated tubes are also present; the tube length is about 100 nm. One end of the individual SWNTs or bundles is usually terminated with an encapsulated particle [Fig. 1(C)], the other with a flat angular cap [Fig. 1(D)] typical of BNNTs.[3,6,14] The most important result stemming from our observations is that SWNT synthesis is possible without a metal catalyst, unlike results obtained from groups that have synthesized SWNTs composed of either carbon or boron nitride.[15,16]

 

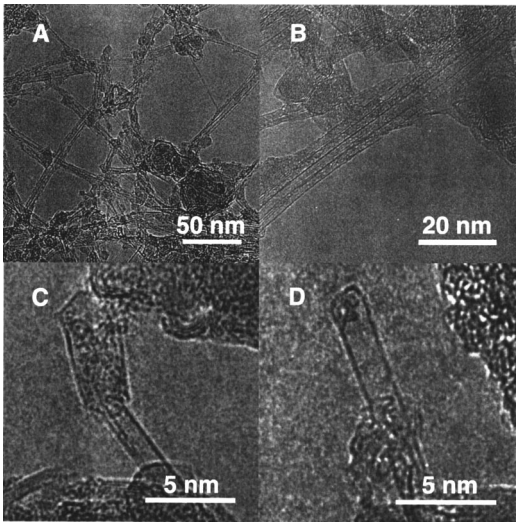


FIG. 1. (A) Low magnification transmission electron micrograph (TEM) of recovered soot, showing bundles of single-wall nanotubes (SWNTs) and a few multiwall nanotubes (primarily double-walled) and nanoparticles. The bundles are composed of ~10 SWNTs and are ~100 nm long. (B) High resolution TEM (HRTEM) of SWNT bundle. (C) HRTEM of the end of a nanoparticle-terminated SWNT. (D) HRTEM of angular or squared off cap of SWNT.

Analysis of the high resolution transmission electron micrographs (HRTEMs) of the SWNTs reveals a diameter distribution centered at 1.6 and 1.4 nm for ''bundled'' and isolated tubes, respectively. The diameters for tubes in bundles were calculated assuming the van der Waals distance between tube walls to be 0.34 nm, as in hexagonal BN (hBN). The diameter distribution for tubes in bundles is very sharp, with a FHWM about 0.3 nm, in contrast with the broader distribution found for isolated tubes with a FWHM about 0.6 nm. The origin of these differences is, as yet, unclear, although it is reasonable that tubes of similar diameter are more likely to form bundles. Our results seem to indicate the existence of a well-defined diameter for which stacking of nanotubes into bundles is favored. It is also interesting to note that the mean diameter of the bundled tubes is similar although slightly larger than the mean diameter ($\simeq 1.4$ nm) of bundled carbon SWNTs (CSWNTs).[15]

Figure 2 shows the boron and nitrogen elemental maps of the sample, obtained using electron energy loss spectroscopy (EELS) imaging in a Philips Tecnai 20F field emission gun TEM. Inelastic electrons corresponding to energy losses $\Delta E = 188$ eV (boron *K*-edge) and $\Delta E = 401$ eV (nitrogen *K*-edge) have been used. The particles terminating the SWNTs only appear in the boron distribution image [Fig. 2(A)], which indicates that they are composed of pure boron. In contrast, nanotubes and fullerenelike structures appear in both the boron and nitrogen elemental maps, and according to quantitative EELS analysis, the boron to nitrogen ratio in these structures is approximately unity. Thus, EELS analysis reveals that the sample is composed of BNNTs, the majority of which are SWNTs terminated by pure boron particles covered with BN ''cages.'' Thus the most important feature of our results is that BNNTs seem to grow from pure boron

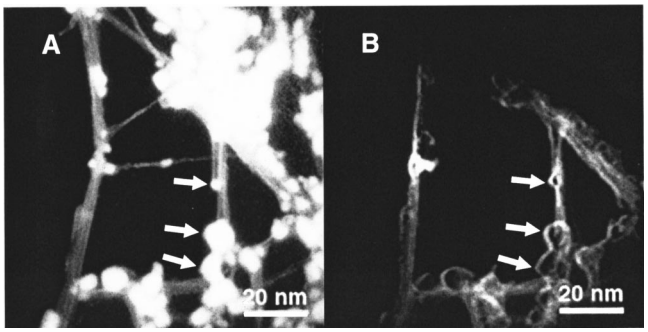


FIG. 2. Elemental maps of boron (A) and nitrogen (B) obtained using EELS imaging with inelastic electrons corresponding to energy losses $\Delta E = 188$ eV and $\Delta E = 401$ eV (boron and nitrogen *K*-edges, respectively). The view in (B) is of the same region as (A) and has been recorded after the view in (A). A few tubes are seen in (A) and not in (B) because they have been destroyed by the electron beam during the time interval separating the recordings of views (A) and (B). The white arrows indicate boron nanoparticles encapsulated in a single BN layer shell.

particles. This strongly suggests a ''root-based'' growth mechanism that will be discussed at the end of this paper in relation with atomistic simulations.[17]

We also succeeded in determining the helicity of the BNNTs by analyzing very high resolution transmission electron micrographs (VHRTEM) obtained with a JEOL 4000EX TEM. The nanotube inside the frame shown in Fig. 3(A) exhibits a dot contrast consistent with a zig-zag configuration.[18,19] This dot contrast is only observable on the wall closest to the bottom of the image, the other wall being screened by the adjacent tube, and is enlarged in Fig. 3(B). It consists of a periodic sequence of dark lobes at the tube image edge, which are elongated perpendicularly to the tube axis; this periodic array being bordered by two white lines. The periodicity of these dark lobes is 0.21 nm and corresponds to the periodicity of the $(10\bar{1}0)$ planes of hexagonal BN. Image simulations have been performed with the EMS code[20] for different tube configurations and are presented in Figs. 3(C)–3(E). They show that only zig-zag BNNTs exhibit a lobe sequence readily comparable to the experimental images. Moreover, these simulations have also shown that regardless of defocus conditions and their corresponding contrast inversions, the black spots lining the walls of the tubes remain a permanent signature of zig-zag BNNTs. Thus, these dark spots are ideal for determining whether BNSWNTs are zig-zag or not. This is a particularly important point to emphasize since these dark dots at the edges are easy to observe in contrast with the full contrast of the BNNT. In fact this last contrast is made of an array of white and black dots which directly reveals the atomic configuration of the BNNTs but unfortunately is very weak and highly sensitive to the orientation of the tubes and to defocus conditions. The majority (85%) of the tubes that we analyzed was of zig-zag type. A minority were either of armchair or chiral type. Since none of these two last types exhibits a signature as clear as that of the zig-zag tubes, their identity remains unclear. However, the salient result of this careful helicity analysis is that most of the tubes are of zig-zag configuration.

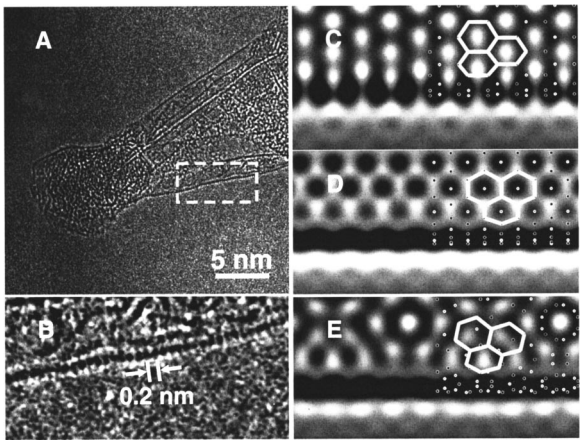


FIG. 3. Helicity analysis of BNSWNTs. (A) HRTEM of BNSWNTs emerging from a boron nanoparticle. The exterior wall of the nanotube at the bottom of the image (area within the frame) exhibits a dotted contrast which are a signature of zig-zag BNNTs; the interior wall is screened by the adjacent BNNTs. (B) Magnification of the area in the frame (A). (C), (D), (E) Simulated images of BNSWNT respectively zig zag – (20,0) configuration – armchair – (12,12) configuration and chiral – (8,16) configuration – calculated using the EMS software with appropriate parameters to simulate the imaging conditions of a JEOL 4000EX (400 kV, Cs $=1$ mm, focus spread$=8$ nm, divergence angle$=0.7$ mrd); the focus is close to the Scherzer focus ($-55$ nm). The simulated images display along the tube wall (or edge) dark lobes due to the (1010) planes, similar to the those in (A) and (B). B (N) atoms are indicated by small white (dark) dots whereas the positions of the B–N bonds are indicated by tick marks in the image. The ''interior'' of the tube exhibits a periodic array of either black or white dots, which are located at the center of the BN hexagons. The contrast of these dots is very weak and highly sensitive to defocus conditions and to the tube diameter.

The fact that we observed predominantly zig-zag BNSWNTs gives us some indication on their growth mechanism. *Ab initio* molecular dynamics simulations have indeed shown[17] that open tips of BNSWNTs with a zig-zag configuration are unstable and tend to form amorphouslike caps, unlike armchair tubes. This instability indicates that the growth of zig-zag BNSWNTs is not possible via an open-ended mechanism without a catalyst. This result together with the fact that the tubes are terminated at one end with a boron nanoparticle supports a ''root-based'' growth mechanism, similar to that initially proposed for the growth of CSWNTs.[21,22] In our case, the metal-carbide particle is replaced by a boron-rich particle (liquidlike or solid). The incoming boron and nitrogen atoms are incorporated into the BN honeycomb network at the bottom or the ''root'' of the tube, where the bonds are most reactive owing to the presence of defects, as schematized in Fig. 4. During the ablation of the target, the BN material is believed to decompose into elemental boron and nitrogen ions, which later reagglomerate to form boron particles and later BNNTs. The complete decomposition of BN at the first stage of the reaction is supported by the results of similar BNNT syntheses performed using boron powder, which show that BNNT synthesis from elemental boron in a nitrogen atmosphere is possible.[23]

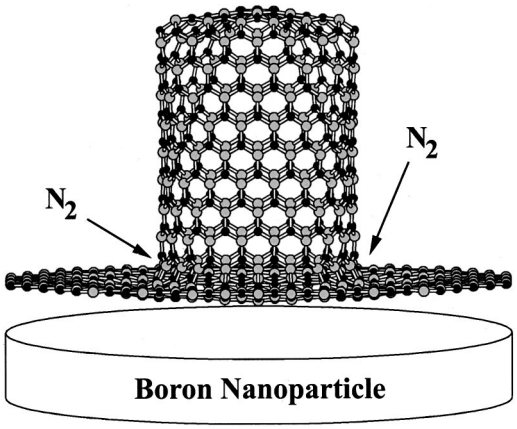


FIG. 4. Schematic view showing the proposed ''root-based'' growth mechanism of BNNTs consistent with our experimental observations. Black and white spheres indicate boron and nitrogen atomic positions, respectively. Tube growth originates from a pure boron nanoparticle created by the decomposition of boron nitride. Boron from the particle reacts with nitrogen in the atmosphere to form a boron nitride nanotube. Nanotube growth proceeds via the introduction of boron and nitrogen atoms at its root.

In conclusion, we have succeeded in synthesizing SWNTs without using a metal catalyst and furthermore we have demonstrated that it is possible to synthesize them in bulk quantities. TEM and EELS analyses have shown that the SWNTs are composed of boron nitride; a vast majority has a zig-zag configuration and they are organized in crystalline bundles. The end of the BNNTs with encapsulated boron nanoparticles and the zig-zag configuration of the majority of the tubes suggests that BNNT grow via a ''root-based'' mechanism.

We would like to thank B. Freitag of the FEI Company (the Netherlands) for his assistance with the Philips Tecnai 20F field emission gun TEM and F. Ducastelle for stimulating discussions. This work was partially supported by a grant from the French Ministry of Foreign Affairs (Bourse Chateaubriand) and CNRS.

[1] A. Rubio, J.L. Corkill, and M.L. Cohen, Phys. Rev. B **49**, 5081 (1994).
[2] N.G. Chopra *et al.*, Science **269**, 966 (1995).
[3] A. Loiseau, F. Willaime, N. Demoncy, G. Hug, and H. Pascard, Phys. Rev. Lett. **76**, 4737 (1996).
[4] D. Golberg *et al.*, Appl. Phys. Lett. **69**, 2045 (1996).
[5] D.P. Yu *et al.*, Appl. Phys. Lett. **72**, 1966 (1998).
[6] M. Terrones *et al.*, Chem. Phys. Lett. **259**, 568 (1996).
[7] J. Cumings and A. Zettl, Chem. Phys. Lett. **316**, 211 (2000).
[8] N.G. Chopra and A. Zettl, Solid State Commun. **105**, 297 (1995).

[9] X. Blase, A. Rubio, S.G. Louie, and M.L. Cohen, Europhys. Lett. **28**, 335 (1994).
[10] J.W. Mintmire *et al.*, J. Phys. Chem. Solids **54**, 1835 (1993).
[11] T. Laude, Y. Matsui, A. Marraud, and B. Jouffrey, Appl. Phys. Lett. **76**, 3239 (2000).
[12] The reactor is a cylindrical, metallic, water-cooled chamber. Nitrogen gas is introduced at the bottom of the chamber and escapes via a silica tube above the target. Reaction products are collected after the tube at two points: an air-cooled metallic trap and a filter [Proceedings of the XIII International Winterschool, Kirchberg, Tirol, Austria, 27 February - 6 March 1999, edited by H. Kuzmany, J. Fink, M. Mehring, S. Roth (American Institute of Physics, New York, 1999)].
[13] The composition of the target (wt. %) was 91.2% boron nitride, 4.0% oxygen, 0.1% calcium, 4.5% $B_2O_3$ and 0.2% other impurities.
[14] A. Loiseau *et al.*, Carbon **36**, 743 (1998).
[15] A. Thess *et al.*, Science **273**, 483 (1996).
[16] G.W. Zhou, Z. Zhang, Z.G. Bai, and D.P. Yu, Solid State Commun. **109**, 555 (1999).
[17] X. Blase, A. De Vita, J.-C. Charlier, and R. Car, Phys. Rev. Lett. **80**, 1666 (1998).
[18] D. Golberg *et al.*, J. Appl. Phys. **86**, 2364 (1999).
[19] D. Golberg, Y. Bando, K. Kurashima, and T. Sato, Chem. Phys. Lett. **323**, 185 (2000).
[20] P. Stadelmann, Ultramicroscopy **21**, 31 (1987).
[21] A. Maiti, C.J. Brabec, and J. Bernholc, Phys. Rev. B **55**, R6097 (1997).
[22] J. Gavillet *et al.* (unpublished).
[23] Synthesis was carried out using boron powder (grain size $=150$ $\mu$m, 99.6% pure); with the exception of the nature of the target, the synthesis conditions were identical to those used for the BN targets. There was no perceptible difference in the quality of these samples as compared to the ones synthesized with the BN target.